# Spatially localized generation of nucleotide sequence-specific DNA damage

**Dennis H. Oh*†‡, Brett A. King§, Steven G. Boxer§, and Philip C. Hanawalt¶**

*Department of Dermatology, University of California, San Francisco, CA 94143; †Dermatology Research Unit, San Francisco Veterans Administration Medical Center, 4150 Clement Street, San Francisco, CA 94121; and Departments of §Chemistry and ¶Biological Sciences, Stanford University, Stanford, CA 94305

Contributed by Philip C. Hanawalt, August 3, 2001

**Psoralens linked to triplex-forming oligonucleotides (psoTFOs) have been used in conjunction with laser-induced two-photon excitation (TPE) to damage a specific DNA target sequence. To demonstrate that TPE can initiate photochemistry resulting in psoralen–DNA photoadducts, target DNA sequences were incubated with psoTFOs to form triple-helical complexes and then irradiated in liquid solution with pulsed 765-nm laser light, which is half the quantum energy required for conventional one-photon excitation, as used in psoralen + UV A radiation (320–400 nm) therapy. Target DNA acquired strand-specific psoralen monoadducts in a light dose-dependent fashion. To localize DNA damage in a model tissue-like medium, a DNA–psoTFO mixture was prepared in a polyacrylamide gel and then irradiated with a converging laser beam targeting the rear of the gel. The highest number of photoadducts formed at the rear while relatively sparing DNA at the front of the gel, demonstrating spatial localization of sequence-specific DNA damage by TPE. To assess whether TPE treatment could be extended to cells without significant toxicity, cultured monolayers of normal human dermal fibroblasts were incubated with tritium-labeled psoralen without TFO to maximize detectable damage and irradiated by TPE. DNA from irradiated cells treated with psoralen exhibited a 4- to 7-fold increase in tritium activity relative to untreated controls. Functional survival assays indicated that the psoralen–TPE treatment was not toxic to cells. These results demonstrate that DNA damage can be simultaneously manipulated at the nucleotide level and in three dimensions. This approach for targeting photochemical DNA damage may have photochemotherapeutic applications in skin and other optically accessible tissues.**

Psoralens are a class of furocoumarins that are widely used in combination with UV A radiation (UVA, 320–400 nm) to treat a variety of skin disorders. One well-studied mechanism of action of this type of photodynamic therapy involves intercalation of psoralen at 5′-TpA-3′ sites in cellular DNA, followed by UVA-induced photochemistry that sequentially results in monoadducts and interstrand crosslinks between psoralen and DNA (1, 2). As with other DNA-damaging agents, psoralens create lesions that are distributed among numerous sites throughout the genome and in numerous cells and tissue layers, resulting in undesirable genotoxic effects to cells (3–5). In addition to damaging DNA and other intracellular targets relatively indiscriminately, conventional photochemotherapy is also limited by the depth of tissue penetration. In skin, for example, the penetrance of light is governed by wavelength-dependent reflection, scattering, and absorption, resulting in minimal penetration of UV relative to that of longer wavelengths (6). Thus, irradiation of deeper targets requires more irradiation to superficial tissue. The combined effects of nonspecific photochemically mediated DNA damage result in acute toxicities as well as an increased risk for malignancy (5).

Recently, the ability of triple helix-forming oligonucleotides (TFOs) to bind specifically to defined DNA sequences via Hoogsteen base pairing with purine-rich strands has generated considerable interest for modifying genomes of cells in a sequence-specific fashion (7–10). Although TFOs alone are site-specifically mutagenic (11, 12), when linked to photochemically active molecules such as psoralens, they can act with even greater control because covalent chromosomal DNA damage can be initiated in cells at a well-defined time by using UVA irradiation (13, 14). We have previously used psoralens linked to TFOs (psoTFOs) to target psoralen photoadducts to the human collagenase gene, which is abnormally overexpressed in various inflammatory and malignant cutaneous disorders (15, 16). In tissues such as the skin, which have a stratified architecture and discrete layers, the ability to selectively damage cells and tissues in both a gene-specific and a spatially specific manner would be important to optimize a therapeutic effect while minimizing toxicity.

One approach for activating photodynamic molecules in a particular volume of condensed media, including biological tissue, is to exploit multiphoton excitation. Simultaneous multiphoton excitation occurs when a molecule absorbs two or more photons whose energies individually are insufficient to cause an electronic transition but whose combined energies correspond to the energy gap between two molecular states (17). Although two-photon absorption probabilities of molecules are very small relative to one-photon absorption cross sections, they are quadratically proportional to the intensity of incident light. Thus, two-photon excitation (TPE) can become significant and even practical with the high fluences achievable with pulsed lasers. By using pulsed and focused laser beams, it becomes possible to use multiphoton absorption to excite fluorophores in a spatially restricted manner. This phenomenon has extensive applications in microscopic imaging as well as the potential for creating optical storage devices (18, 19). Multiphoton excitation of biological molecules resulting in DNA damage has also been reported (20–24). However, due to the relatively low probability of TPE during a molecular collision, multimolecular photochemistry with macromolecules after TPE has rarely been directly demonstrated *in vitro* (23) or in cells, although it has been inferred from downstream biological effects (24, 25), including cytotoxicity from TPE of psoralens (22).

We and others have previously documented that the excited state of the psoralen, 4′-hydroxymethyl-4,5′,8-trimethylpsoralen (HMT), is accessible by near-infrared (NIR) light with a quadratic power dependence that indicates a two-photon process (22, 26). After either one- or two-photon excitation, the resulting emission spectra were nearly identical, suggesting that although the selection rules for the two processes are formally different,

BIOPHYSICS

Abbreviations: CPD, cyclobutane pyrimidine dimer; HMT, 4′-hydroxymethyl-4,5′,8-trimethylpsoralen; NIR, near-infrared; TFO, triple helix-forming oligonucleotide; psoTFO, psoralen conjugated to TFO; TPE, two-photon excitation; UVA, UV A radiation (320–400 nm).

‡To whom reprint requests should be addressed at: Dermatology Service (190), Veterans Administration Medical Center, 4150 Clement Street, San Francisco, CA 94121. E-mail: doh@orca.ucsf.edu.

The publication costs of this article were defrayed in part by page charge payment. This article must therefore be hereby marked "*advertisement*" in accordance with 18 U.S.C. §1734 solely to indicate this fact.

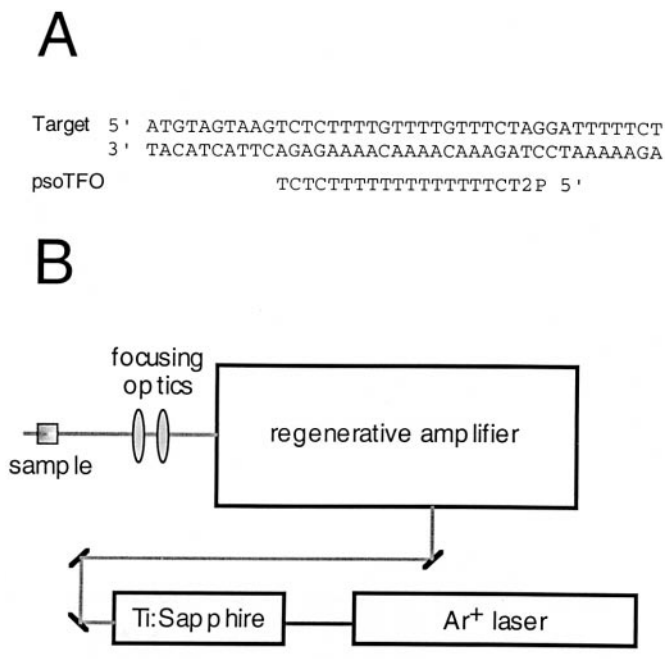


**Fig. 1.** (*A*) psoTFO and duplex DNA target. In the TFO sequence, C represents 5-methyl-C, and P represents 4′-hydroxymethyl-4,5′,8-trimethylpsoralen linked at the 4′-hydroxymethyl group to the TFO via a two-carbon aliphatic chain. The last two residues at the 3′ end of the TFO are phosphorothioates; the remainder are phosphodiesters. (*B*) Schematic diagram of TPE laser irradiation apparatus.

evolution to the same emitting and potentially chemically reactive excited states could occur. NIR TPE of psoralens and other photodynamically useful drugs offers several advantages over conventional excitation, including greater depth of tissue penetration due to reduced scattering of longer wavelengths, manipulation of the spatial selectivity of the photodynamic effect through the use of focused or intersecting laser beams, as well as minimal absorption from nonpharmacologic chromophores in the skin (6).

Here we report that TPE creates psoralen adducts with DNA in cells, that the psoTFO adducts can be targeted to specific DNA sequences, and that the damage can be preferentially targeted to a three-dimensional region within a model tissue phantom. The results suggest that TFOs, when tethered to photodynamically active compounds, can provide sequence specificity, whereas multiphoton excitation of these reagents can provide spatial specificity, significantly enhancing their potential to deliver photodynamic DNA damage to genomic and cellular targets without deleterious collateral damage.

## Materials and Methods

**Materials.** Oligodeoxyribonucleotides were obtained as HPLC-purified reagents (Oligos Etc., Wilsonville, OR) and have been previously described in detail (15, 16). Briefly, the DNA target was formed by annealing complementary 40-bp sequences corresponding to a segment of the human interstitial collagenase gene (Fig. 1*A*). psoTFO4 is a psoTFO that possesses a phosphodiester backbone except for two phosphorothioate residues at the 3′ terminus. The 5′ terminus was modified with a two-carbon linker conjugated to HMT. psoTFO4 was routinely handled in dim yellow light (>500 nm) to avoid unintentionally activating the psoralen moiety. Unconjugated HMT and [$^3$H]-labeled HMT (HRI Associates, Concord, CA) were stored as ethanolic solutions at −20°C until used.

**Formation of Noncovalent Triple Helical Complexes.** psoTFO4 (33 $\mu$M) was incubated with duplex target DNA (5 $\mu$M) in binding buffer (10 mM Tris, pH 7.5/20 mM $MgCl_2$/1 mM spermidine) at 22°C for 1 h before the start of irradiation in a 1-mm path-length quartz cuvette. For experiments in polyacrylamide gels, the complex of psoTFO and duplex target was similarly formed initially in liquid solution, followed by addition and polymerization of 40% (wt/vol) acrylamide in binding buffer, resulting in a solution that contained 6.8 $\mu$M duplex target/40 $\mu$M psoTFO4/10% polyacrylamide in binding buffer. The 1-cm$^3$ gel was allowed to polymerize in a 1-cm pathlength polystyrene cuvette (Bio-Rad) for 2 h at 22°C before the start of irradiation.

**Irradiation.** The UVA source was a planar array of BL lamps (Ultraviolet Products) in a housing of local design, as previously described (15, 16). As shown in Fig. 1*B*, TPE experiments used the pulsed output of a regenerative amplifier (762–770 nm, 140-to 200-fs pulse duration, 450- to 700-mW average power, 1-kHz pulse frequency, Spitfire, Positive Light, Santa Clara, CA) seeded with a titanium/sapphire laser (762–770 nm, ≈140-cm $^{-1}$ bandwidth, ≈110-fs pulse duration, 1-W average power, 82-MHz pulse frequency, Tsunami, Spectra-Physics) that was pumped by an $Ar^+$ laser (6–10 W, all lines, Spectra-Physics). The 450- to 700-mW average laser power at the sample corresponded to peak powers of $\approx 3.5 \times 10^9$ W. Most TPE experiments were conducted with a 5-mm-diameter collimated laser beam that passed through liquid reaction solutions held in a 1-mm pathlength quartz cuvette. Experiments designed to localize DNA damage spatially were conducted by expanding the laser beam diameter in a diverging lens, followed by focusing in a convex lens. The converging beam was focused through a 1-cm$^3$ gel formed in a cuvette. Beam diameters were measured visually with a millimeter ruler. Calculations based on experimentally measured diameters assume a homogeneous intensity throughout the beam, and no attempt is made to correct for a Gaussian or otherwise inhomogeneous beam profile.

**Assay for psoTFO Adducts.** The gel mobility-shift assay has previously been described (15, 16, 27). After irradiation of liquid reaction mixtures, 5-$\mu$l aliquots were subject to analysis. After irradiation of reaction mixtures formed in a polyacrylamide gel, the gel was carefully extricated from its plastic cuvette and visually sectioned by hand into thirds in each dimension with a no. 11 surgical blade, resulting in 27 volume elements or voxels. The estimated error in the dimension of a voxel's side was ±1 mm. DNA from each voxel was extracted with 100-$\mu$l buffer (10 mM Tris, pH 7.5/1 mM EDTA) for 2 h at 37°C, and then each voxel was re-extracted with 100 $\mu$l of water at 4°C overnight; the extracts were then pooled. DNA was precipitated from sample solutions with ice-cold ethanol in the presence of 0.3 M sodium acetate, washed in 70% ethanol, and end-labeled with $^{32}$P by using T4 polynucleotide kinase (Life Technologies, Gaithersburg, MD). The end-labeled products were then precipitated with ethanol and separated under denaturing conditions with 6% PAGE. The dried gel was then imaged by autoradiography and quantified by phosphorimaging (GS-360, Bio-Rad). All stages of sample preparation and analysis were performed in dark or dim yellow light. In some cases, the data were numerically modeled by using KALEIDAGRAPH 3.05 (Abelbeck Software, Reading, PA).

**Assay for Psoralen Adducts in Cells.** Normal human dermal fibroblasts originally prepared from neonatal foreskin were grown to confluence on no. 2 glass microscope cover slips (VWR Scientific) in Fibroblast Growth Medium (Clonetics, Walkersville, MD) supplemented with 5% FBS. Fifteen minutes before irradiation, cells were washed with PBS and then immersed in 1 $\mu$M HMT with or without tritium label in 1:1 (vol/vol) PBS/Hanks'

buffered saline solution in a locally designed glass cuvette with a Delrin insert capable of holding 14 coverslips for simultaneous irradiation in a laser beam. With all 14 coverslips in place in the cuvette and immersed in solution, the transmission through the cuvette was 70% (data not shown). The cuvette was placed in a collimated laser beam and irradiated at room temperature for 13 h. Control cells were treated identically but were not irradiated. After irradiation, the cells were washed and examined under phase-contrast microscopy. Cells from all coverslips were then released with 0.05% trypsin, pooled, and lysed in 0.5% SDS in buffer (10 mM Tris, pH 7.5/1 mM EDTA). DNA was prepared from the lysate by using a commercial column (DNeasy, Qiagen, Chatsworth, CA) and then adsorbed onto DE-81 paper (Whatman), washed extensively with PBS to remove any remaining unbound HMT, dried, and quantified by liquid scintigraphy (Beckman). To determine cellular survival after treatment, identically treated and irradiated cells were washed in PBS and incubated at 37°C with 0.05% (wt/vol) thiazolyl blue in fibroblast growth medium containing 5% FBS for 3 h (28). The colored precipitate was then dissolved in dimethyl sulfoxide and spectrophotometrically quantified at 540 nm.

## Results

**Two-Photon Excitation Generates psoTFO Photoadducts *in Vitro*.** To demonstrate the ability of TPE to initiate psoralen photochemistry, psoTFO4 was added to liquid solutions of its double-stranded target and then irradiated with UVA or laser. As shown in Fig. 2*A*, unirradiated samples possessed two bands (lanes 2 and 7). The upper and lower bands correspond to the pyrimidine- and purine-rich target strands, respectively (16). In the presence of UVA, two products are detectable in addition to the unreacted single-stranded DNA, corresponding to monoadduct formation of the psoTFO with only one target strand, and an interstrand crosslink corresponding to adduct formation with both target strands (lane 1). In the presence of 760 nm of light, a single product is observed that corresponds to monoadducts and depends on light dose (lanes 2–5). No crosslinked product was detectable at any irradiation time up to 13 h. At 13 h of irradiation, ≈25% of the DNA had reacted. As shown in Fig. 2*B*, under constant irradiation, the rate of monoadduct formation is modeled nicely with pseudofirst-order kinetics, as expected for a system in which the psoTFO is in large molar excess and forms a 1:1 noncovalent complex with its DNA target. For the experimental conditions studied, the rate constant derived from such modeling is $1.4 \times 10^9$ s $^{-1}$. To ensure that these products did not result from reactions associated with the DNA target itself or from single-photon excitation of a contaminant that resulted in adduct or crosslink formation, DNA target alone in solution was irradiated with either UVA (Fig. 2*A*, lane 6) or with laser for identical times (lane 8) and did not result in any detectable products. No reaction is evident when either a random sequence psoralen–oligonucleotide or a random sequence DNA target is used (data not shown and refs. 15 and 16).

**Spatial Localization of DNA Damage.** The ability to localize psoTFO damage was investigated by forming noncovalent psoTFO/DNA target complexes in a polyacrylamide gel that restricted mobility of the reactants and products during and after irradiation. The gel was formed in a polystyrene cuvette that was placed in a converging laser beam (Fig. 3*A*). The focal point was placed behind rather than in the gel to avoid photoionization at the extremely intense focus of the unattenuated laser beam. The beam diameters at the front and rear outer faces of the cuvette were 8 and 4 mm, respectively. When corrected for beam displacements due to refractive index changes, the diameters at the front and rear of the gel were 7.6 and 4.3 mm, respectively.[‖] After 13-h irradiation, the gel remained optically clear without visible distortion. The cubic gel was sectioned into 27 smaller cubes measuring 3 ± 1 mm per side, and the products were analyzed by gel-shift mobility assay (Fig. 3*B*). As in liquid solution, the products were entirely monoadducts between the

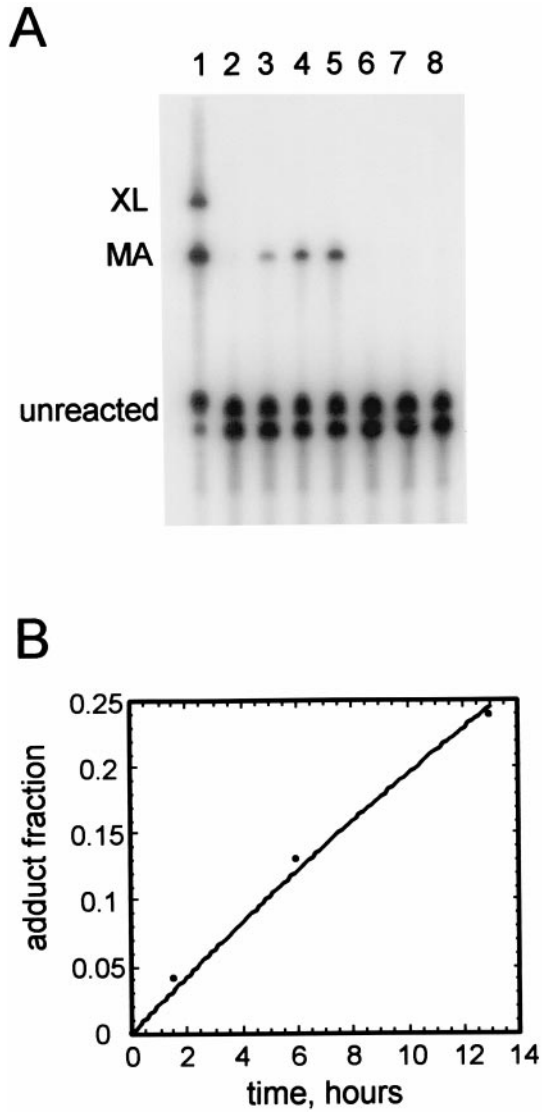


**Fig. 2.** Formation of psoTFO adducts with target DNA. (*A*) Target DNA was incubated with psoTFO4. The mixture was then irradiated either with 0.15 J/cm$^2$ UVA (lane 1) or with 765-nm laser for 0, 1.5, 6, and 13 h (lanes 2–5, respectively). Target DNA in the absence of psoTFO4 was also irradiated with 0.15 J/cm$^2$ UVA (lane 6) or with 760-nm laser for 0 or 13 h (lanes 7 and 8, respectively). Reaction products were labeled with $^{32}$P at their 5′ termini, separated on a denaturing 6% polyacrylamide gel and detected by autoradiography. MA and XL indicate targets covalently linked to the psoTFO via HMT monoadducts or interstrand crosslinks, respectively. (*B*) Quantitative analysis of lanes 2–5 was performed by using phosphorimaging, and data were then modeled with a first-order kinetic model, $[MA]/[DNA]_0 = (1 - e^{-kt})$, where $[MA]/[DNA]_0$ represents the fraction of total DNA targets converted to monoadducts, and $k$ is the pseudofirst-order rate constant of the reaction.

[‖] Snell's law was used to calculate internal angles and beam diameter corrections within the cuvette. The refractive index for 10% polyacrylamide was approximated by that of water (1.33). The refractive indices for air and polystyrene are 1.00 and 1.59, respectively (29). The dimensions of the cuvette's walls and internal pathlength used for these calculations were confirmed by using a micrometer.

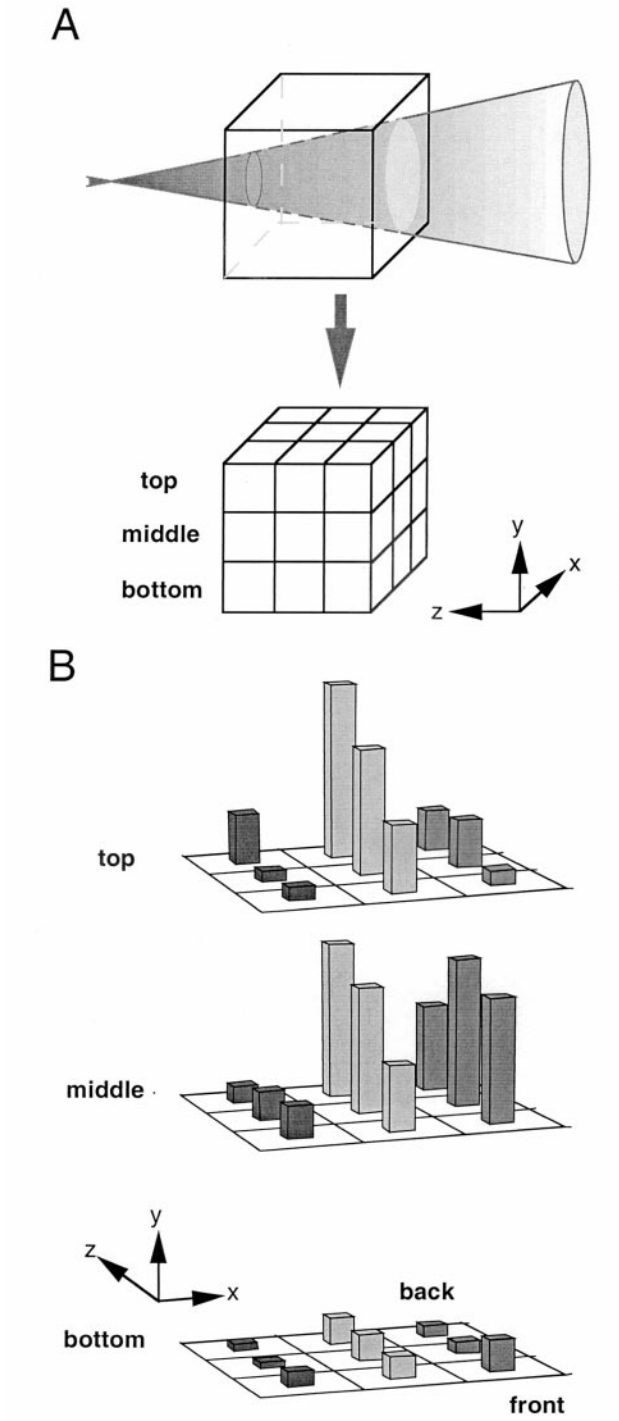


**Fig. 3.** Preferential formation psoTFO adducts in three dimensions. (*A*) Schematic diagram of irradiation of psoTFO4 and target duplex complexes in a polyacrylamide gel. The laser beam was focused to a point behind the center of the gel. After irradiation, the gel was sectioned into voxels, and products were analyzed. (*B*) Results of gel mobility-shift assay for each voxel oriented in three-dimensional space. Each bar represents the fraction of DNA in each voxel that migrated as a monoadduct. The tallest bar represents 33% of the total DNA. Note the view orientation has been rotated clockwise about the *y* axis by 70° to clearly show all data points.

TFO and the purine-rich strand of the duplex target (data not shown). Most of the damage was concentrated in the top and middle of the central *yz* plane of the gel, indicating that the laser beam either was not centered on the *y* axis or was not cross-sectionally homogeneous. The middle *yz* plane, especially in the top and middle thirds, displayed a trend of increasing damage from front to back. In the rear central voxels, up to 33% of targets were damaged, in contrast to 13% in the front voxels, with the middle voxels possessing intermediate levels of damage. Off-axis voxels in the gel did not have significant levels of damage, with the exception of the middle-right voxels, which had levels of damage ranging from 15 to 28% with no particular trend. Overall, summing over all voxels in the front and rear, the percentage of total available targets damaged in the rear third of the gel was 14% in contrast to 10% in the front third.

**Table 1. Two-photon excitation of HMT in cultured fibroblasts**

| Sample | % survival | Relative $^3$H activity |
|---|---|---|
| Untreated | 98 | 0 |
| HMT | 94 | 1 |
| HMT + laser, sample no. 1 | 99 | 4 |
| HMT + laser, sample no. 2 | | 7 |

**Two-Photon Excitation Generates Photoadducts in Cells.** Although targeted psoTFO adducts do form in cells after UVA irradiation (15), they are sufficiently low in abundance that detection of their presence in cells after an infrequent TPE event was difficult. Thus, to increase the amount of damage signal, normal human fibroblasts were treated with free HMT that reacts with multiple sites in the genome. Fibroblasts irradiated with 760 nm of light for 13 h had a 4- to 7-fold increase in tritium activity associated with their nucleic acid in comparison with unirradiated cells (Table 1). These results indicated that HMT covalently associated with nucleic acid as a result of TPE. Cellular density and morphology were not visibly altered under phase-contrast microscopy. Cellular survival 13 h after the start of irradiation was not significantly diminished in the presence of HMT alone or in cells treated with HMT and laser irradiation. Results indicate that TPE is capable of forming adducts with genomic DNA in cells without producing acute toxicity.

## Discussion

TPE and TFOs have previously been individually used to damage DNA. TPE using 810-nm femtosecond laser pulses has been reported to induce cyclobutane pyrimidine dimers with DNA alone as well as strand breaks when irradiating DNA in the presence of proflavine (23). There have also been multiple reports of cells treated with TPE either alone or in the presence of a photosensitizer that have inferred the creation of DNA damage from changes in cellular or subcellular morphology or survival but that have not directly demonstrated such damage (21, 22, 24, 25, 30). Many of these downstream biological or morphological effects may result from secondary effects of the irradiation, such as through generation of reactive oxygen species that randomly damage DNA (30). In contrast, TFOs have been used with or without chemically reactive agents to target damage and subsequent mutations to cellular DNA with great specificity (15, 31, 32). However, TFO technology alone does not allow control over which tissues or cells within a particular tissue will have their DNA targeted with site-specific damage. For example, TFOs administered systemically can induce mutations in multiple tissues (12). Therefore, because TPE by its physical nature is capable of concentrating photochemical DNA damage to a preferential volume of space, and TFOs by their chemical nature are capable of placing photodynamic agents at a specific nucleotide in a genome, the combination of these two approaches has potential for manipulating DNA damage in both physical space and nucleotide sequence.

We and others have previously reported that psoralens have a measurable two-photon cross section at NIR wavelengths produced by a titanium/sapphire laser (22, 26). However, this earlier work did not demonstrate actual DNA damage. In the current study, we report that HMT either alone or conjugated to a TFO is capable of forming adducts with DNA. NIR irradiation of psoTFOs with target DNA results exclusively in monoadducts. No interstrand crosslinks formed, consistent with previous observations that psoralens preferentially form monoadducts when excited at the red edge of their absorption spectrum (33–36). These results indicate that NIR TPE and single-photon UVA irradiation, although formally possessing different selection rules for electronic transitions, excite HMT to electronic states that evolve to similar if not identical photochemically reactive states. The photochemistry of protoporphyrin IX has also been observed to be similar after either one- and two-photon absorption (37).

When incubated with psoTFO4, ≈25% of the starting target material converted to monoadducts over 13 h, corresponding to a pseudofirst-order rate constant of $1.4 \times 10^9\ s^{-1}$. This result can be compared with an expected yield by using a previously published equation for the rate ($R$) of TPE-induced photochemistry (22):

$$R = \frac{\delta \cdot C \cdot P_{pk} \cdot P_{avg} \cdot \Phi}{2 \cdot A}.$$

$R$ is described in terms of the TPE cross section ($\delta$), concentration ($C$), peak laser power ($P_{pk}$), average laser power ($P_{avg}$), laser beam cross-sectional area ($A$), and the quantum yield of photochemistry ($\Phi$). We have previously measured $\delta$ for HMT in ethanolic/aqueous solution at 730 nm to be 20 Göppert–Mayer (G-M) (26) (1 G-M = $10^{-50}$ $cm^4 s$). In the current set of experiments, by using a regenerative amplifier, it was necessary to use a longer wavelength at 765 nm. It appears that $\delta$ varies with wavelength approximately proportionally to the corresponding one-photon absorption for a psoralen closely related to HMT (22). Thus, because the one-photon absorption of HMT at 382.5 nm is 16.1% of that at 365 nm (26), a value for $\delta$ at 765 nm can be estimated from the HMT absorption spectrum to be 3.2 G-M. $\Phi$ has been determined from one-photon experiments on HMT to be 0.016 for monoadduct formation (38). These values, along with the experimental parameters described earlier, may be used to estimate a TPE-induced reaction rate of $6.7 \times 10^9\ s^{-1}$. The total possible target DNA reactants contained in our 5-$\mu$M 75-$\mu$l solution is $2.25 \times 10^{14}$, and thus after 13 h, the rate equation predicts 100% conversion to adducts, larger than our experimental measurement of 25% conversion. However, the rate equation used above must be regarded as only a crude approximation to the experimental situation reported here, because it was derived with the assumption that reactant concentrations are negligibly affected during the reaction. Other approximations used in the above estimates include equating irradiation of the entire volume of reactants with irradiation of only a portion of the reaction vessel, assuming $\delta$ is identical in ethanolic/aqueous and purely aqueous solutions and ignoring cross-sectional heterogeneity in the intensity of the laser beam. Given these simplistic and possibly incorrect assumptions, the observation that the experimental and predicted reaction rates are within a factor of four is surprisingly good and also suggests that the quantum yield for monoadduct formation by HMT is similar after both one- and two-photon irradiation.

TPE has been widely used for three-dimensional microscopic imaging by using a variety of fluorophores (18). TPE has also been investigated as an approach for creating optical memory storage devices (19, 39) and has been suggested as a potential tool for selectively activating photochemotherapeutic agents in tissue (22, 24, 26). Psoralens, as well as other photodynamic agents used for cutaneous therapy, represent fortuitously attractive targets for TPE with NIR radiation, because skin is the most optically accessible tissue of the body, and these wavelengths are within a spectral window where absorption from melanin and other skin chromophores as well as water is at a minimum (6). To determine whether TPE can be used to localize psoTFO adducts in three-dimensional space, we used a model system in which psoTFOs were allowed to noncovalently bind to their DNA targets in an acrylamide solution, which was then allowed to polymerize into a cubic gel to minimize diffusion during laser irradiation. The laser beam was allowed to converge such that the cross-sectional area at the front of the gel was twice that at the rear of the gel, resulting in a higher beam intensity at the rear. Clearly, some beam misalignment or inhomogeneity existed, resulting in an unexpected number of off-axis adducts in the middle gel section. However, as predicted for TPE-induced photochemistry, within the central voxels of the gel through which the axis of the laser beam passed, the number of adducts formed at the rear was significantly higher than at the front.

Quantitatively, because TPE probability is quadratically related to the incident light intensity, one predicts that the adduct density within the laser beam at the very rear of the gel would be larger than that at the very front. Experimentally, the gel was sectioned approximately into thirds in each dimension, resulting in 27 individual voxels. The theoretical adduct density in each fully irradiated voxel is therefore calculated by integrating the square of beam intensities through each third of the gel along the beam axis.** The ratio of expected intensities results in a predicted ratio of rear/front adduct densities of 4.6. A 1-mm error in front and rear gel sections results in a predicted range of possible adduct density ratios of 2.5–8.6. Our measured ratios in the central voxels (2.6–2.8), although lower than that predicted for a gel perfectly sectioned into thirds, fall within the range of experimental error and are consistent with TPE-induced adducts. If the overall number of adducts in each third of the gel is examined, TPE in our experimental configuration is expected to produce 2.2-fold more adducts in the rear than in the front third of the gel, in contrast to one-photon excitation, which should produce equivalent numbers of adducts in each third of the gel. The experimental observation that the rear third of the gel possessed 40% more adducts than the front is therefore also consistent with TPE. These results are proof-of-principle that TPE can preferentially localize photodynamic DNA damage in three-dimensional space and that, with psoTFOs, such damage can also simultaneously be localized to a particular DNA sequence.

To demonstrate that TPE can be used to create DNA damage in cells without resulting in acute nonspecific toxicity from thermal or photoacoustic effects, we treated cells with [$^3$H]-HMT and irradiated under the same conditions used to generate TPE-induced psoTFO adducts on model DNA oligomers. Relative to untreated or unirradiated controls, these cells had significantly more tritium counts associated with their DNA, indicating that HMT had covalently reacted with the cell's DNA as a result of TPE. Equally important, cells so treated were metabolically active and normal in morphology relative to controls after a 13-h treatment, suggesting that the treatment itself was not immediately toxic. Others have demonstrated toxicity, either through cell death or by morphological changes indicative of apoptosis (22, 37).

**The integrated probability of TPE, $P_{TPE}$, along a direction $z$ from an initial position $z_i$ to a final position $z_f$ in a gel irradiated by a laser beam of power, $W$, with a convergence angle of $2\theta$ is given by:

$$\int_i^f P_{TPE} dz = \frac{W^2}{3\pi^2 \tan^4\theta} \cdot \left(\frac{1}{z_i^3} - \frac{1}{z_f^3}\right).$$

However, such experiments used high repetition rates (80 MHz) that may have resulted in thermal damage. Our experiments used a regenerative amplifier with an output frequency of 1 kHz, which allowed a higher peak power as well as sufficient time for thermal equilibration with the surrounding medium.

It has also been reported that 810-nm femtosecond pulses on plasmid DNA can result in cyclobutane pyrimidine dimers (CPD) detected enzymatically, although the mechanism by which this occurs is unclear (23). We cannot exclude that such DNA damage occurred in our system, but the unaltered mobility of oligomers irradiated in the absence of psoTFOs suggests that it did not. Furthermore, the wavelength of our laser would not allow irradiation into the absorption bands responsible for CPD formation through a two-photon mechanism. Although a three-photon mechanism is possible in principle, its probability is expected to be even smaller than that for TPE, rendering it a small, if not negligible, fraction of the total products generated at this wavelength.

This work was supported by the National Institutes of Health through Mentored Clinical Scientist Development Award K08-AR02008 (D.H.O.), Outstanding Investigator Grants CA44349 (P.C.H.) and GM27738 (S.G.B.), and by Air Force Office of Scientific Research Grant F49620–00-1–0349.

1. Cimino, G. D., Gamper, H. B. & Hearst, J. E. (1985) *Annu. Rev. Biochem.* **54,** 1151–1193.
2. Gasparro, F. P. (1988) in *Psoralen DNA Photobiology*, ed. Gasparro, F. P. (CRC, Boca Raton, FL), Vol. 1**,** pp. 5–36.
3. Sage, E. & Moustacchi, E. (1987) *Biochemistry* **26,** 3307–3314.
4. Nataraj, A. J., Black, H. S. & Ananthaswamy, H. N. (1996) *Proc. Natl. Acad. Sci. USA* **93,** 7961–7965.
5. Stern, R. S., Laird, N., Melski, J., Parrish, J. A., Fitzpatrick, T. B. & Bleigh, H. L. (1984) *N. Engl. J. Med.* **310,** 1156–1161.
6. Anderson, R. R. & Parrish, J. A. (1981) *J. Invest. Dermatol.* **77,** 13–19.
7. Sun, J.-S., Garestier, T. & Helene, C. (1996) *Curr. Opin. Struct. Biol.* **6,** 327–333.
8. Maher, L. J. (1996) *Cancer Invest.* **14,** 66–82.
9. Chan, P. P. & Glazer, P. M. (1997) *J. Mol. Med.* **75,** 267–282.
10. Vasquez, K. M. & Wilson, J. H. (1998) *Trends Biochem. Sci.* **23,** 4–9.
11. Wang, G., Levy, D. D., Seidman, M. M. & Glazer, P. M. (1995) *Mol. Cell. Biol.* **15,** 1759–1768.
12. Vasquez, K. M., Narayanan, L. & Glazer, P. M. (2000) *Science* **290,** 530–533.
13. Giovannangeli, C., Diviacco, S., Labrousse, V., Gryaznov, S., Charneau, P. & Hélène, C. (1997) *Proc. Natl. Acad. Sci. USA* **94,** 79–84.
14. Majumdar, A., Khorlin, A., Dyatkina, N., Lin, F.-L. M., Powell, J., Liu, J., Fei, Z., Khripine, Y., Watanabe, K. A., George, J., Glazer, P. M. & Seidman, M. M. (1998) *Nat. Genet.* **20,** 212–214.
15. Oh, D. H. & Hanawalt, P. C. (1999) *Nucleic Acids Res.* **27,** 4734–4742.
16. Oh, D. H. & Hanawalt, P. C. (2000) *Photochem. Photobiol.* **72,** 298–307.
17. Göppert-Mayer, M. (1931) *Ann. Phys.* **9,** 273.
18. Denk, W., Strickler, J. H. & Webb, W. W. (1990) *Science* **24**.
19. Parthenopoulos, D. A. & Rentzepis, P. M. (1989) *Science* **245,** 843–845.
20. Leupold, D. & Kochevar, I. E. (1997) *Photochem. Photobiol.* **66,** 562–565.
21. Calmettes, P. P. & Berns, M. W. (1983) *Proc. Natl. Acad. Sci. USA* **80,** 7197–7199.
22. Fisher, W. G., Partridge, W. P., Dees, C. & Wachter, E. A. (1997) *Photochem. Photobiol.* **66,** 141–155.
23. Shafirovich, V., Dourandin, A., Luneva, N. P., Singh, C., Kirigin, F. & Geacintov, N. E. (1999) *Photochem. Photobiol.* **69,** 265–274.
24. Berns, M. W., Wang, Z., Dunn, A., Wallace, V. & Venugopalan, V. (2000) *Proc. Natl. Acad. Sci. USA* **97,** 9504–9507.
25. Shea, C. R., Hefetz, Y., Gillies, R., Wimberly, J., Dalickas, G. & Hasan, T. (1990) *J. Biol. Chem.* **265,** 5977–5982.
26. Oh, D. H., Stanley, R. J., Lin, M., Hoeffler, W. K., Boxer, S. G., Berns, M. W. & Bauer, E. A. (1997) *Photochem. Photobiol.* **65,** 91–95.
27. Gasparro, F. P., Havre, P. A., Olack, G. A., Gunther, E. J. & Glazer, P. M. (1994) *Nucleic Acids Res.* **22,** 2845–2852.
28. Mosmann, T. (1983) *J. Immunol. Methods* **65,** 55–63.
29. Weast, R. C. (1978) *Handbook of Chemistry and Physics* (CRC, West Palm Beach, FL).
30. Tirlapur, U. K., König, K., Peuckert, C., Krieg, R. & Halbhuber, K. J. (2001) *Exp. Cell. Res.* **263,** 88–97.
31. Wang, G., Seidman, M. M. & Glazer, P. M. (1996) *Science* **271,** 802–804.
32. Belousov, E. S., Afonina, I. A., Kutyavin, I. V., Gall, A. A., Reed, M. W., Gamper, H. B., Wydro, R. M. & Meyer, R. B. (1998) *Nucleic Acids Res.* **26,** 1324–1328.
33. Chatterjee, P. K. & Cantor, C. R. (1978) *Nucleic Acids Res.* **5,** 3619–3633.
34. Gasparro, F. P., Saffran, W. A., Cantor, C. R. & Edelson, R. L. (1984) *Photochem. Photobiol.* **40,** 215–219.
35. Shi, Y. B. & Hearst, J. E. (1987) *Biochemistry* **26,** 3792–3798.
36. Gasparro, F. P., Gattolin, P., Olack, G. A., Deckelbaum, L. I. & Sumpio, B. E. (1993) *Photochem. Photobiol.* **57,** 1007–1010.
37. Goyan, R. L. & Cramb, D. T. (2000) *Photochem. Photobiol.* **72,** 821–827.
38. Hearst, J. E. (1981) *J. Invest. Dermatol.* **77,** 39–44.
39. Parthenopoulos, D. A. & Rentzepis, P. M. (1990) *J. Appl. Phys.* **68,** 5814–5818.